Chemical Engineering Science, Vol. 49, No. 2, pp. 223–232, 1994.
Printed in Great Britain.

0009–2509/94 $6.00 + 0.00

THE GASIFICATION OF WOOD-CHAR SPHERES IN CO_2–N_2 MIXTURES: ANALYSIS AND EXPERIMENTS

S. DASAPPA,[†] P. J. PAUL,[‡] H. S. MUKUNDA[‡§] and U. SHRINIVASA[‖]
[†]ASTRA, [‡]Department of Aerospace Engineering, [‖]Department of Mechanical Engineering, Indian Institute of Science, Bangalore 560012, India

(*Received* 11 *May* 1992; *accepted for publication* 14 *July* 1993)

Abstract—The gasification of charcoal spheres in an atmosphere of carbon-dioxide–nitrogen mixture involving diffusion and reactions in the pores is modelled and the results are compared with experiments of Standish and Tanjung and those performed in the laboratory on wood-char spheres to determine the effects of diameter, density, gas composition and flow. The results indicate that the conversion time, $t_c \sim d^{1.03}$ for large particles (> 5 mm), departing substantially from the $t_c \sim d^2$ law valid for diffusion limited conditions. The computational studies indicate that the kinetic limit for the particle is below 100 μm. The conversion time varies inversely as the initial char density as expected in the model. Predictions from the model show that there is no significant change in conversion time up to 60% N_2 consistent with the CO_2–N_2 experiments. The variation of diameter and density with time are predicted. The peculiar dependence of conversion time on flow velocity in the experiments is sought to be explained by opposing free and forced convection heat transfer and the attempt is only partly successful. The studies also indicate that the dependence on the CO concentration with low CO_2 is significant, indicating the need for multistep reaction mechanism against the generally accepted single-step reaction.

1. INTRODUCTION

Gasification of charcoal has been reported by several researchers, with the emphasis on design of reactors, furnaces and cupolas, where either coal, charcoal or wood is used as the fuel. In all these applications, the combustion/gasification of the char after devolatisation is an important process. While conversion of char in air at ambient condition or oxygen rich condition is known to be diffusion limited, the importance of kinetics is felt in the reduction reactions involved in the gasification process. Wood charcoal, known for its high reactivity, has been studied much less than coal char for the evaluation of either the kinetic parameters or conversion times in well-defined geometries. Most of the earlier work on char gasification has been done on the coal char and on small particles in the range of 0.02–1.5 mm diameter. Most of the experimental studies (Ergun, 1956; Blackwood and Ingeme, 1960; Dutta *et al.*, 1977; Kasaoka *et al.*, 1985; DeGroot and Shafizadeh, 1984; Muhlen *et al.*, 1985) are directed towards a packed-bed gasification, with very limited work on single particles (Groeneveld and Swaaij, 1980; Mukunda *et al.* 1984; Standish and Tanjung, 1988). Reyes and Jensen (1986a, b) have carried out work on the char particles in the range around 200 μm, using percolation of gas into the porous char involving enlargement and coalescence of the pores, and particle disintegration at high porosity. Morell *et al.* (1990) have carried out a model study for char gasification of 100 μm char particles in a mixture containing multispecies. The model uses a fact that the particle disintegration occurs at a critical conversion, beyond which particle size variation takes place.

1.1. *Kinetic studies*

Blackwood and Ingeme (1960), in their detailed analysis of the reaction mechanism, quote an expression of Semechkova and Frank-Kamenetskii who derived the following volumetric rate expression from a (assumed) multistep scheme:

$$\dot{\omega}_c''' = -\frac{k_1 p_{CO_2} - k_2 p_{CO}^2}{1 + k_3 p_{CO} + k_4 p_{CO_2}}. \quad (1)$$

They made careful experiments at various pressures on coconut char and indicate that the expression (1) is satisfactory at atmospheric pressures but needs improvement at high pressures to account for methane formation. They derived a new expression, which differs from eq. (1) in the second term in the numerator, to account for the high pressure behaviour and obtained the rate constants in the kinetic expression. An advantage of the expression (1) is that the equilibrium limit is preserved. It is possible that the non-linear term is unimportant, as considered by many authors. In most of the other kinetic studies on coal char or wood charcoal gasification (DeGroot and Shafizadeh, 1984; Kasaoka *et al.*, 1985; Sundaresan and Amundson, 1979), the rate expressions are either fitted to the experimental data using a single-step-reaction mechanism with power law for mass fraction dependence or have large number of parameters to be fitted with the experimental results. The overall order of the reaction is taken to be around 0.6–0.7. The lower order of the reaction is an approximation to the variation of the order from 1 to 0 for CO_2 mass fractions changing from near zero mass fractions to near unity. Some workers (DeGroot and Shafizadeh, 1984; Kasaoka *et al.*, 1985; Sundaresan and Amundson, 1979) use rate expressions containing carbon concentration. This approach of relating to the carbon concentration is not greatly appealing since

[§]Author to whom correspondence should be addressed.

the heterogeneous reaction depends on the surface area rather than on the concentration of the condensed phase.

Satyanarayana and Keairns (1981) in their review state that only the initial rate of carbon gasification reactions has been investigated in detail and the change in rate with carbon conversion has been studied very little. In most of the cases the initial 10% of the conversion is used for evaluating the kinetic parameters, the results of which do not indicate the changes in the rate with conversion. They also derive a rate expression for the C–CO_2 reaction by ignoring the non-linear term in the numerator and unity in the denominator of eq. (1). The latter feature will be shown to be inaccurate as other terms are not as large as presumed at low concentrations of CO_2. In any case, there does not appear any serious justification for such a simplification when relatively more complete expressions have already been developed.

1.2. *Single-particle studies*

Ergun (1956) studied the C–CO_2 kinetics using a fluidised-bed configuration on activated carbon and graphite, and deduced (by involved arguments based on availability of active sites) that there is no dependence of the reactivity on particle size in the size range 0.08–1.8 mm. Groeneveld and Swaaij (1980) have conducted experiments using slices of wood charcoal placed in a reactor with the reactant CO_2 (17% and temperature 1173 K) flowing on the top surface to obtain the conversion profiles. The experiments are restricted to a carbon conversion of 40%. Their one-dimensional mathematical model ignores the variation of temperature in the porous char. The model was shown to give good comparison of conversion with experiments except beyond a certain distance from the surface. It is shown in the present work that over the distances of the kind used in the experiments of Groeneveld and Swaaij (35 mm), the approximation of constant temperature breaks down at high CO_2 concentrations and becomes better at lower concentrations; even so, the rates differ by a factor of two due to temperature and 10 due to concentrations at free-stream mole fraction of 17% of CO_2. A further point of criticism on the rate equation is that the rate of conversion is independent of whether the species is CO_2 or H_2O. They use a rate expression as

$$-R_A = kC_s(C_{CO_2} + C_{H_2O})^{0.7} \qquad (2)$$

where k is the rate constant, C_s is the concentration of solid (carbon), C_{CO_2} and C_{H_2O} are, respectively, the molar concentrations of CO_2 and H_2O. However, data from Blackwood and Mcgrory (1958), Kasaoka *et al.* (1985) and Satyanarayana and Keairns (1981) show that H_2O is far more reactive than CO_2. It is puzzling that, in this otherwise carefully conducted study, the reactivities of H_2O and CO_2 are made equal.

Reyes and Jensen (1986a, b) treat the problem of char–gas reactions including diffusion using percolation theory. The model treats pore space topology in detail including particle disintegration processes. The application seems to involve cases where the initial porosity is very small. This is seen to lead to pressure gradient through the pore. The pressure through the pores evens out with conversion. At the range of porosity considered in the present work (80% and beyond) their theory indicates fragmentation. Several of the processes described in their work are weakly relevant to the current work. Morell *et al.* (1990) investigate the char reaction with several species (CO_2, H_2O, O_2 and H_2) using a single-step mechanism for the heterogeneous reaction. The parametric study explores particle radii up to 500 μm with steam as primary reactant gas and to be the effect of ambient pressure. While many results of calculation are presented without any experimental support, there appears no explanation for the minimum in conversion time with particle size.

Standish and Tanjung (1988) have conducted experiments on wood-char spheres of 10–20 mm diameter in an atmosphere of CO_2–N_2 at varying temperatures and composition. The measurements of weight loss with time have been carried out till near complete conversion. This work has a number of interesting and useful results not adequately analysed. While the data of conversion time with temperature, CO_2 mass fraction, and diameter dependence are all consistent with both reaction and diffusion being important as shown subsequently, the data of density and diameter with conversion are not. Their argument that the conversion is governed by shrinking core model, their correlation which has the character of kinetic control and part of their data which clearly shows significant kinetic control are internally inconsistent. In their experiments on flow effects, the total conversion time shows a peak with gas velocity, a feature which is acknowledged by them as unexplainable even qualitatively.

Experiments and modelling studies on wood-char combustion in air have been conducted by Mukunda *et al.* (1984) to determine and predict the burn time of the large diameter particles in the range 10–20 mm. Although the model predicted the burn time with reasonable accuracy, the predicted core temperature was as high as 1400 K and the measured values were about 1100 K. This is argued to be due to the neglect of C–CO_2 reaction in the model and the need to model the C–CO_2 reaction properly. This is one of the motivations for the present study.

2. THE PRESENT WORK

The review of the earlier work indicates that (a) the basic kinetic results have not been integrated into a model including non-isothermal behaviour to explain the experimental results, (b) the interesting results of Standish and Tanjung (1988) need to be replicated experimentally and explained based on a rigorous model, and (c) the long standing results of Ergun (1956) that wood char up to 1.8 mm exhibits independence on particle size have neither been confirmed nor challenged.

The present work is devoted to study the C–CO_2 reaction using the detailed mechanism obtained by Frank-Kamenetskii. Such a study was found essential as the reaction mechanism of char with carbon dioxide is different from that of char with air presented in Mukunda *et al.* (1984). This work is also essential as the kinetics of char with H_2O and O_2 is dependent on CO_2 (fraction) which is formed during the above set of reactions. It will be shown that the use of detailed chemistry is essential while considering the mixture of gaseous species with lower reactant concentration. Thus, this work essentially aims at conducting critical experiments to replicate some of the earlier experimental data, particularly with regard to flow effects, and improving the theoretical model developed at the laboratory (Mukunda *et al.*, 1984) for understanding and explaining the results of the above studies.

2.1. *The experiments*

Experimental set-up (shown in Fig. 1) consists of a quartz reactor of 40 mm diameter placed in a temperature controlled furnace. The reactant gas was heated to the furnace temperature before letting into the reactor by passing the gas through a helical quartz tube wound round the reactor. The flow rate of the gas was measured using a capillary flow meter calibrated by water displacement technique. The experimental procedure was similar to that of Standish and Tanjung (1988). The sample was suspended from a balance inside the reactor maintained at the required temperature and the reactant gas was passed through the reactor. The variation of mass of the sample with time, the total conversion time, and the mass flow rate of the gas were recorded. In some experiments only the conversion time and the gas flow rate were recorded.

The particle size of the samples was in the range 3.5–15 mm. Char samples were prepared in two different ways: by burning dried wood spheres in air and quenching them at the end of flaming combustion or by slow heating of wood spheres in the absence of oxygen. The charcoal spheres obtained were dried in an oven at 373 K for more than 24 h and weighed after cooling in a desiccator. The char samples were dried again in the oven for 8 h, cooled and weighed. The sample was considered dry if there was no difference between the weights at two different times. In some cases, the char samples were finished to obtain spherical geometry. The density of char obtained by fast pyrolysis was 180 ± 20 kg/m^3 and that obtained by slow pyrolysis was 400 ± 30 kg/m^3. The second method appears to be the one followed by Standish and Tanjung. One particular difficulty experienced was the purity of CO_2 obtained from outside. To purify the CO_2, the gas cylinder was chilled using liquid nitrogen to solidify CO_2, evacuated to remove the residual impurities like O_2 and N_2 and later brought back to ambient temperature.

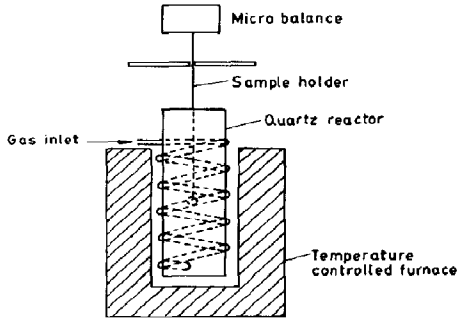

Fig. 1. Experimental set-up.

During the experiments it was observed that the char sphere was nearly of the same size till about 50–70% burn time when the ash layer covering the sphere was noticed. However, the carbon core was visible through the ash layer till the end of the burn time. Towards the end of the run the ash used to fall off from the sphere in many cases. The experiments were limited to reactor temperature of 1273 K and 100% CO_2 and were conducted to confirm the results of Standish and Tanjung. If there was confirmation, it was thought appropriate to use their data over a wider range of parameters for comparison.

Measurements were made on particle diameter, weight and the surface area based on BET technique at different conversions. SEM pictures of the surface as well as the core were taken at different conversion levels. The ash content in the char is between 4–5%. The result of the ash analysis is as follows, SiO_2 (1.1%), Al_2O_3 (7.5%), CaO (19.4%), MgO (22.1%) and P_2O_5 (9.6%).

2.2. *The model*

The processes taking place during the combustion or gasification of porous carbon spheres are: (1) diffusion and convection of the species and energy in the porous medium, and (2) heterogeneous reaction between the gaseous species and the char. These are modelled in the present analysis using the unsteady spherically symmetric one-dimensional conservation equations. The conservation equations are

$$\frac{\partial}{\partial t}(\rho\varepsilon Y_i) = \frac{1}{r^2}\frac{\partial}{\partial r}\left(-\rho v r^2 Y_i + r^2 D_e \rho \frac{\partial}{\partial r} Y_i\right) + \dot{\omega}_i''' \tag{3}$$

$$\frac{\partial \varepsilon}{\partial t} = -\dot{\omega}_c'''/\rho_c \tag{4}$$

$$\frac{\partial}{\partial t}(\bar{\rho} c_p T) = \frac{1}{r^2}\frac{\partial}{\partial r}\left(-\rho v r^2 c_p T + r^2 k \frac{\partial T}{\partial r}\right) - H_c \dot{\omega}_c''' \tag{5}$$

where $\bar{\rho} = \rho_c(1-\varepsilon) + \rho\varepsilon$ is the average density of porous char, ρ_c is non-porous char density, ε is the porosity of the char and $\dot{\omega}_c'''$ is the volumetric reaction rate of char. The subscript $i = 1, 2, 3$ refers to species CO, CO_2 and N_2, respectively. A rate expression similar to eq. (1) is used for calculating the reaction rate. This expression neglects the surface area variation with conversion and, as mentioned earlier, the data of first 10% of conversion time has been used to

derive the constants of eq. (1). Hence, in the present work the reaction rate at any conversion has been obtained as $\dot{\omega}_c''' = \dot{\omega}_{c0}''' S_g/S_{g0}$, where $\dot{\omega}_{c0}'''$ is the volumetric reaction rate at zero conversion and S_g the surface area per unit volume of char. The internal surface area per unit volume is related to the porosity and pore radius according to Howard (1967) by $S_g = 2\varepsilon/r_p$ and $\dot{\omega}_c''' = \dot{\omega}_c'' S_g$.

In deriving the above expression, the mechanism of overlap and intersection of growing pores have been neglected. More sophisticated model is not used because the change in surface area with conversion is not significant for wood char of high initial porosity.

Plates 1 and 2 show the scanning electron micrographic pictures of wood char at 0 and 65% conversion. The geometric order present in these pictures is remarkable. One can notice long tubes in the 0% conversion case; the tubes show the longitudinal section of the char. The 65% case shows the cross section of the char, a bee-hive like network having dimensions of the order of 20–30 μm. These constitute the cell walls and the hollow section region of converted carbon. These are similar to the SEM pictures obtained by Standish and Tanjung (1988). These pictures are to be contrasted with those on coal char in Dutta *et al.* (1977); they indicate highly random structures and

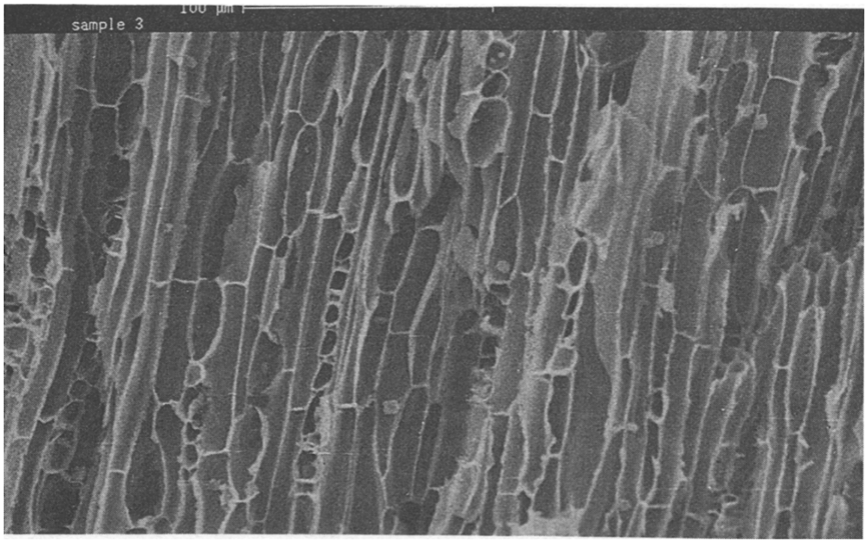

Plate 1.

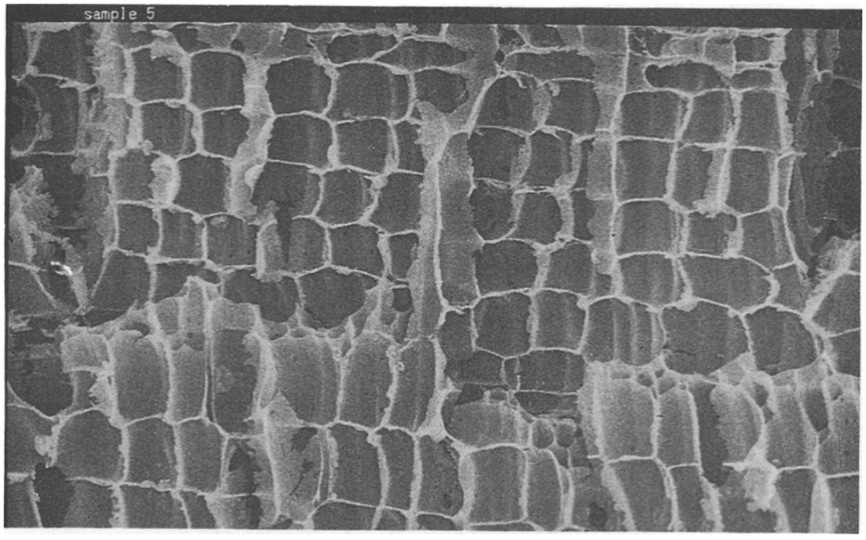

Plate 2.

holes. The difference between the regular structures in wood char and the irregular ones in coal char is due to their origin. Coal is the highly treated form of biomass under pressure and heat and therefore the order found in wood cannot be expected to be retained in coal. This aspect makes many of the aspects of random pore structure theories less relevant to wood char conversion. The wood char samples were also characterised for the pore surface area using the BET technique. In doing the experiments all the sample (broken into a few pieces because of the limitation of the sample holder) was used in the apparatus. Thus, the total surface area at certain level of conversion was obtained. These data are converted into surface area per unit volume using the dimensions of the char. Figure 2 shows a typical plot of the surface area per unit volume as a function of the conversion. It can be seen that it weakly varies with conversion. This feature is consistent with the information that can be derived from the SEM pictures. A simple-minded calculation of the pore surface evolution assuming a square holed structure with a web shows that the surface area increases by about 10% at an initial porosity of 80%. The surface area will linearly increase till burn out at which point the entire structure will collapse suddenly. Earlier literature has some points supporting this aspect. Gavalas (1981) indicates that the relative increase in the surfae area and diffusion coefficient is much larger when the initial porosity is small. In a comment on this paper (of Gavalas), Simons (1981) interprets the results as implying that the effect of coalescence of the pore mouths is negligible for porosities characteristic of carbon chars during combustion (0.2 to 1.0). Thus, the simple model of pore size increasing with time without any coalescence is adequate for wood chars considered in this study.

The variation of pore radius r_p with time is obtained by treating the pores as long tubes from the relation of Howard (1967):

$$\rho_c \frac{\partial r_p}{\partial t} = -\dot{\omega}_c''. \tag{6}$$

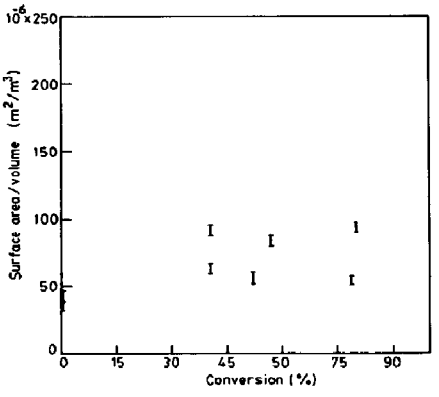

Fig. 2. Variation of surface area per unit volume of char with conversion.

The diffusion coefficient of the gaseous components in the porous medium is given by Howard (1967), $\bar{D}_e = D\varepsilon/\tau$, where τ and D are the tortuosity factor and the effective diffusivity, respectively (Howard, 1967).

$$\frac{1}{D} = \frac{1}{D_k} + \frac{1}{D_g}, \quad \text{where } D_k = \frac{2r_p}{3}\left(\frac{8RT}{\pi M_g}\right)^{1/2} \tag{7}$$

where D_k and D_g are the Knudsen and gas diffusion coefficients respectively and r_p is the pore radius. The thermal conductivity of the porous char, $\bar{k}$, which is a function of temperature, is the volumetric average of the solid and gas conductivities, k_c and k_g. Formally it is given by $\bar{k} = k_c(1-\varepsilon) + k_g\varepsilon$.

The gas phase is treated quasisteady. The gas-phase equations are the species and energy governing equations and are given by

$$\frac{\dot{m}c_p}{4\pi r^2}\frac{\partial T}{\partial r} = \frac{1}{r^2}\frac{\partial}{\partial r}\left(kr^2\frac{\partial T}{\partial r}\right) \tag{8}$$

and

$$\frac{\dot{m}}{4\pi r^2}\frac{\partial Y_i}{\partial r} = \frac{1}{r^2}\frac{\partial}{\partial r}\left(D\rho r^2\frac{\partial Y_i}{\partial r}\right). \tag{9}$$

The solution for the above equations, assuming Lewis number as unity, can be written as

$$\frac{T - T_\infty}{T_s - T_\infty} = \frac{Y_i - Y_{i\infty}}{Y_s - Y_{i\infty}} = \frac{1-\eta}{1-\eta_s} \tag{10}$$

where $\eta = e(-\dot{m}c_p/4\pi kr)$. The mass and heat flux thus obtained from the above need to be modified to include free and forced covection by using emperical relations as indicated in Yuge (1960).

2.2.1. *Initial, interface and boundary conditions.* The initial conditions at $t = 0$ are the temperature and concentration profiles within the porous char. The temperature is set at the cold ambient temperature or the temperature of the furnace depends on the experimental condition. The precise nature of the concentration profile does not matter as the transients die down in a small fraction of the conversion time. The interface conditions at $r = r_s$ are one of continuity of heat and mass fluxes. These are (Mukunda *et al.*, 1984)

$$\begin{aligned} D_g\rho\left.\frac{\partial Y_i}{\partial r}\right|_{r_s} &= Q(Y_{i\infty} - Y_{is}) \\ k\left.\frac{\partial T}{\partial r}\right|_{r_s} &= c_pQ(T_\infty - T_s) - \dot{R}'' \end{aligned} \tag{11}$$

where $\dot{R}''$ is the radiative heat flux from the surface of the sphere and

$$Q = \frac{\dot{m}}{4\pi r_s^2}\frac{\exp(-B_0)}{[1-\exp(-B_0)]}, \quad B_0 = \frac{\dot{m}c_p}{2\pi r_s kNu}. \tag{12}$$

Equation (12) is obtained from the solution of spherically symmetric one-dimensional conservation equations for the gas phase (Mukunda *et al.*, 1984) and the effect of free and/or forced convection is accounted for by choosing the appropriate value of the Nusselt

number, Nu. $Nu = 2$ in the absence of either free or forced convection; but increases in presence of convection. In the earlier work (Mukunda *et al.*, 1984), the char sphere encountered only free convection. In the present case, both will be present. Since the C–CO_2 reaction is endothermic, the sphere is at a lower temperature compared to the furnace and experiences negative buoyancy. An examination of the literature revealed that correlations of experimental data on spheres are available in Yuge (1960) for combined free and forced convection. The interesting feature of these experiments and the correlation is that in a narrow range of small Reynolds (Re) and Grashof (Gr) numbers, the net heat transfer rate decreases as Re increases since forced convection acts in opposition to natural convection.

2.3. *Method of solution*

The solution calls for integration of the parabolic system of partial differential equations with the initial and boundary conditions noted above. The independent variable r is transformed into a $\mathscr{V}$ defined as $\mathscr{V} = (4/3)\pi r^3$, making the system of equations fully conservative and removing the singularity at $r = 0$.

The transformed equation for species and energy conservation equation are given by

$$\frac{\partial}{\partial t}(\rho\varepsilon Y_i) = \frac{\partial}{\partial \mathscr{V}}\left[-\dot{m}Y_i + D\rho(4\pi)^{2/3}(3\mathscr{V})^{4/3}\frac{\partial Y_i}{\partial \mathscr{V}}\right] + \dot{\omega}'''_{si} \tag{13}$$

$$\frac{\partial}{\partial t}(\rho\varepsilon T) = \frac{\partial}{\partial \mathscr{V}}\left[-\dot{m}c_pT + k(4\pi)^{2/3}(3\mathscr{V})^{4/3}\frac{\partial T}{\partial \mathscr{V}}\right] + H_c\dot{\omega}'''_{si} \tag{14}$$

where $\dot{m} = (\rho v)_s 4\pi r^2$. For obtaining the mass flow rate of the gases issuing out of the porous char consistent with respect to the unsteady formulation, the equation of state $\rho = PM_g/RT$ is used to obtain

$$\frac{\rho\varepsilon}{\bar{\rho}}\frac{\partial(\rho\varepsilon)}{\partial t} + \frac{1}{\rho}\frac{\partial \varepsilon}{\partial t}\left(1 - \frac{\rho_c\varepsilon}{\bar{\rho}}\right) - M_g\sum\frac{1}{M_i}\frac{\partial(\rho\varepsilon Y_i)}{\partial t} - \frac{\partial(\bar{\rho}c_pT)}{\partial t}\frac{\rho\varepsilon}{c_pT\bar{\rho}} = 0. \tag{15}$$

The mass flow rate $\dot{m}$ in the above equations is a function r (or $\mathscr{V}$) and is evaluated from eq. (15). The integration of the above equations is carried out by using the implicit Crank–Nicholson scheme. The present computations used eight grids. It was ensured that these results are grid independent by obtaining the results for 16 grid points.

2.4. *Choice of parameters*

The choice of physical, thermodynamic and transport properties is based on the mean char properties presented as follows:

$\rho_c = 1900$ kg/m^3 $\quad r_p(t=0) = 50\ \mu$m $\quad c_p = 1.25$ kJ/kg K

$H_c = 32.60$ MJ/kg $\quad k_c = 1.85$ W/m K $\quad k_g = 0.071$ W/m K

$k_1 = 2.2 \times 10^9 e^{-E/RT}$ mol/cm^3 s atm $\quad k_3 = 15.0$ atm^{-1} $\quad k_4 = 0.25$ atm^{-1}

where k_c is the conductivity of the solid phase at temperatures of 1200–1400 K. This leads to porous char conductivity of 0.4–0.5 W/m K obtained from several works (Anon, 1934, Goldman *et al.*, 1984) and accounts for conduction and radiation inside the char. The initial porosity of the wood char was measured experimentally and found to be 0.75–0.85, similar to the values quoted by Groeneveld (1980). An estimate of the initial radius of the pore was obtained from Groeneveld (1980) who has provided photomicrographs of the wood char. The parameters in the kinetic expression used presently are obtained from Blackwood and Ingeme (1960). The rate of the backward reaction k_2 is obtained from the appropriate equilibrium constants.

3. RESULTS AND DISCUSSION

Two principal parameters which influence the solution are the activation energy, E, and char conductivity, $\bar{k}$. The former parameter affects the initial slope of the graph of conversion vs time curve and $\bar{k}$ affects the point at which the curve departs significantly from the linearity. The conductivity value chosen was in the range of values suggested for char and therefore was not altered. The conversion vs time data of Standish and Tanjung (1988) were used to evaluate E. The value of 318 kJ/mol of Blackwood and Ingeme (1960) had to be reduced to 293 kJ/mol to correctly predict the results on ash free basis of Standish and Tanjung (1988). Figure 3 shows the present computational results along with the experimental results of Standish and Tanjung (1988). The difference in E is possibly due to the differences in biomass used. Blackwood and Ingeme (1960) refers to coconut char and Standish and Tanjung (1988) refers to char from Indonesian rubber tree. The presence of small amounts of minerals inevitable in biomass may act as catalysts leading to change in E.

An attempt was made to collapse the experimental data at various temperatures into a single curve using a corrected time t' defined as

$$t' = t\exp\left[-\frac{E_s}{R}\left(\frac{1}{T} - \frac{1}{T_{ref}}\right)\right] \tag{16}$$

where T_{ref} is the reference temperature (chosen as 1173 K), and E_s the superficial activation energy of the gasification process. The best estimate of E_s is obtained as 85 kJ/mol and Fig. 3 also shows the plot of conversion vs the corrected time. The bold line in the right side of Fig. 2 is obtained from computation with $E = 293$ kJ/mol. This good comparison may be thought of as determining E. The difference between the superficial activation energy, E_s, and the true activation energy, E, is due to the diffusional effects.

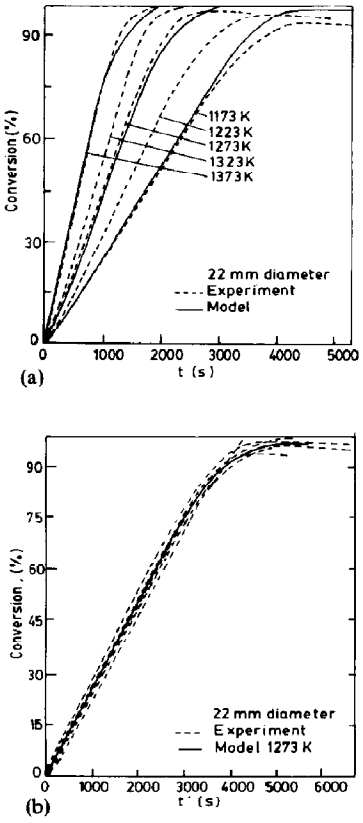

Fig. 3. Data of Standish and Tanjung in original coordinates, and with the corrected time (with temperature), and the present predictions.

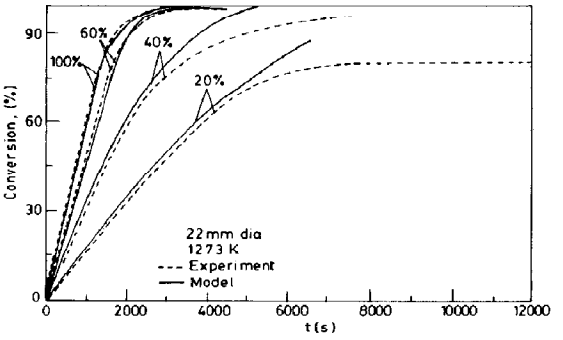

Fig. 4. Original data of Standish and Tanjung along with the predictions of the present model for 100% CO_2, 60% CO_2 + 40% N_2, 40% CO_2 + 60% N_2 and 20% CO_2 + 80% N_2.

The effect of change in ambient CO_2 concentration has been studied by Standish and Tanjung. Figure 4 shows the plot of conversion at $T = 1273$ K for a 22 mm diameter sphere as a function of CO_2 mole fraction. The interesting feature of the plot is that the conversion is weakly dependent on CO_2 mole fraction upto 60%. Below this value there is significant decrease in the conversion rate. Another fact is that conversion seems to asymptote to about 85% at lower mass fractions of CO_2. This feature is evident even with larger CO_2 fractions and at all temperatures. However, in these cases conversion asymptotes at 97%. This is suggested (Standish and Tanjung, 1988) to be due to carbon being locked up in fused ash and being inaccessible for further reaction with CO_2. This phenomenon is one of the dominant processes in rice husk combustion, particularly at high temperatures, but is present even in wood charcoal when the time of reaction is very large. It also depends on the mineral content of the wood. Figure 4 also shows the comparison between predictions and the experimental results. The comparison is excellent up to a conversion of 60%. The relative lack of dependence on the CO_2 ambient concentration upto 60% is due to the nature of the kinetic expression which indicates small dependence of the reaction rate on the mass fraction of CO_2 upto about 60%. The departure of the results beyond 60% conversion is due to ash fusion process discussed above, a feature not modelled in the present analysis. Very little of this occurs at larger mass fractions of CO_2 and is pronounced at lower ambient CO_2 levels. This is argued to be due to the time it takes for the ash fusion to occur. If we hypothesize that the time taken for fusion to occur at a given temperature is about same, then fusion will occur at lower conversion levels at lower ambient CO_2 levels. This is consistent with the observations in the experiments.

Figure 5 shows the experimental data [present as well as Standish and Tanjung, (1988)] and predictions of conversion time with char diameter on a log–log plot. The experimental data are presented assuming a density of 400 kg/m^3. Data for other densities are normalised by noting that $t_c \sim \bar{\rho}$ (consistent with the rate expression used here as well as the exact results for the diffusion-limited case) and consider 90% conversion time as it could be measured more accurately than the complete conversion time. The data presented in Fig. 5 for $\bar{\rho} = 190$ kg/m^3 and $\bar{\rho} = 420$ kg/m^3 bear out this expectation. The predictions are excellent with regard to conversion time. A curve fit of these lead to $t_c/\bar{\rho} = 300d^{1.03}$ (d is the initial diameter in mm) up to particle size of 5 mm. The exponent on the initial diameter is an indication of departure from the diffusion-limited result which leads to quadratic dependence on d and true kinetic limit for which $t_c \sim d^0$. These imply a dual control by diffusion and reaction for the range of conditions considered here. In order to explore the region of true kinetic limit, calculations were extended to lower diameters and the results of conversion time, temperature difference between the surface and the core ($T_s - T_c$), and the ratio of reaction rates at the surface to that at the core and are plotted. The temperature difference comes down to near zero values when $d \sim 100$ μm and the rates at the core and surface become equal. This condition is the precise specification of true kinetic dependence.

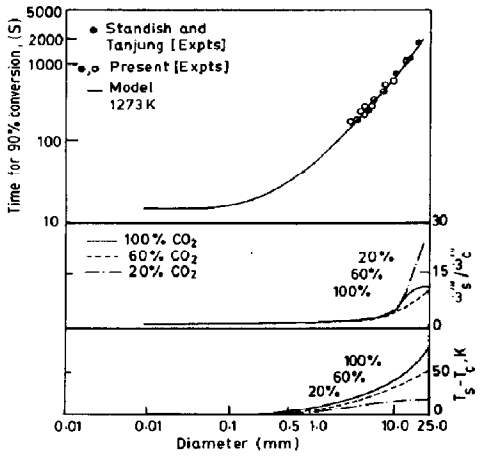

Fig. 5. Variation of time for 90% conversion, ratio of reaction rates at surface to that at the centre, and the temperature difference between the surface and the centre at 30% conversion with particle diameter. The computational results and the experimental results from the present work and from Standish and Tanjung are plotted: (○) density 190 kg/m^3, and (◑), density 420 kg/m^3.

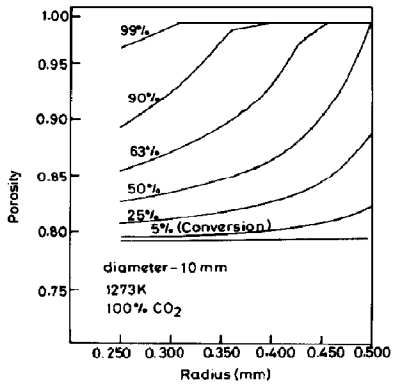

Fig. 6. Plot of porosity with radius at different conversions for a 10 mm char sphere, 1273 K and 100% CO_2 (present).

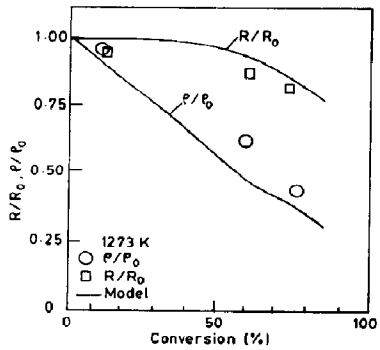

Fig. 7. Plot of conversion vs density ratio and radius ratio for a 10 mm char sphere (present).

Thus, the above result of 100 μm should be contrasted with the result of Ergun (1956) that kinetic limit is approached at 1.8 mm. Even allowing for the fact that coal chars used by Ergun (1956) are likely to be less reactive (and hence diffusion independence might be achieved at a larger diameter) the size quoted for kinetic limit by Ergun appears large. Further, at low CO_2, concentrations one can expect kinetic limit to be achieved at higher diameters. For instance, at 20% CO_2, the kinetic limit is obtained below 350 μm diameter. Many experimenters (Dutta *et al.*, 1977; Kasaoka *et al.*, 1985; DeGroot and Shafizadeh, 1984; Muhlen *et al.*, 1985) who have used particle sizes of 20–80 μm can be understood to have obtained true kinetic dependence. Thus, the limit diameters can be determined from such calculations.

The plot of the variation of the porosity through the sphere with radius, at various conversion levels (or time), is shown in Fig. 6. If the gasification process is kinetic limited, the porosity would increase uniformly with time through out the sphere. On the other hand, in the diffusion limited regime, the reaction takes place in a thin zone and there would be an abrupt change in porosity at the reaction zone, the radius of this zone moving towards the centre with time. The fact that the curves in Fig. 6 show a behaviour between the two extreme cases, the porosity increasing throughout with the rate of change of porosity increasing with r, implies that the process is controlled both by kinetics and diffusion. This, of course, is consistent with the results of Fig. 5.

Figure 7 shows the comparison of the density ratio and radius ratio with conversion. It can be seen that the predictions from the computation compare favourably with those of the experiments, particularly if we note that, in the experiments, lower bound for the radius ratio and upper bound for the density ratio are obtained. Standish and Tanjung (1988) have presented similar results, but seem to have interchanged the nomenclature for density ratio and radius ratio. This inference is due to the following argument. The plot is a reflection of the conversion vs time upto a time when there is significant change in slope. Hence, one would expect a curve with slope near 45° for density ratio and near constant value for radius ratio with conversion upto 40–50%. Because of these considerations their data is not presented here.

An analysis of the importance of the various terms in the rate equation (1) is carried out by obtaining the magnitude of the terms at the peak reaction rate region. One representative set of values is presented in Table 1. It appears from the values of the terms in the numerator of eq. (1), $k_1 p_{CO_2}$ and $k_2 p_{CO}^2$, which are given in Table 1, that the reverse reaction is negligible as is usually assumed. The fact that it has been included here will imply only a thermodynamic completeness. The value of the terms in the denominator, namely, 1, $k_3 p_{CO}$ and $k_4 p_{CO_2}$, show that the second term decreases

Table 1. The value of the terms in the rate expression

Composition		$k_1 p_{CO_2}$	$k_2 p_{CO}^2$	$k_3 p_{CO}$	$k_4 p_{CO_2}$
100% CO_2	Core	0.46×10^{-4}	3.60×10^{-6}	11.7	0.55×10^{-1}
	Surface	6.57×10^{-4}	0.27×10^{-6}	7.05	1.33×10^{-1}
20% CO_2	Core	0.65×10^{-5}	0.79×10^{-6}	3.53	0.12×10^{-2}
	Surface	0.72×10^{-4}	5.90×10^{-5}	2.70	0.10×10^{-1}

from large values at high concentrations of CO_2 to values not too large compared to unity at low concentrations of CO_2. In any realistic situation, where combination of gases in a reactor participate in the gasification reaction, the concentration of CO_2 would be reasonably low. Hence, one cannot ignore the term unity as has been suggested in Satyanarayana and Kearns (1981). Similar arguments rule out the use of single-step reaction mechanism advocated by Groeneveld and Swaaij (1980), Dutta *et al.* (1977) and others. The modification of the reaction rate expression in the present work [eq. (1)] by including the change in surface area due to increase in porosity leads to reaction rate changes of no more than 6%. This change in the rate reduces the conversion time by less than 3%.

3.1. *Flow effects*

Figure 8 shows the experimental results on flow effects from the present work for 10 mm diameter and from Standish and Tanjung (1988) for sphere diameters in the range of 19–25 mm (average 22 mm) on conversion time vs *Re* plot. It is noticed that the conversion time has a peak in both the experiments, albeit at different *Re*. This is qualitatively consistent with the results of *Nu* dependence on *Gr* and *Re* given by Yuge (1960) where, the minimum *Nu* occurs at different *Re* depending on *Gr*. However, the predictions of the model using Yuge's correlations for 22 mm sphere show that, though a peak in burn time is predicted, the magnitude of the peak is very small compared to the experimental observations—of the present work or of Standish and Tanjung (1988). An analysis of the contribution to the modes of heat transfer showed that radiation contributes only 1% of the total flux to the surface. Thus, the convective mode of heat transfer was reexamined. The maximum decrease in *Nu* from its value at $Re = 0$ obtained by Yuge is about 0.5. In order to explain the experimental observations a decrease in *Nu* of at least two is required. For a large part of the gasification time the sphere experiences *Gr* outside the limits of validity Yuge's correlations (for $0.39Gr^{0.25} < 1.0$). Further, the blowing on the sphere surface could cause an early separation of flow from the surface causing reduction in heat (and mass) transfer coefficients (Jaluria, 1980). Thus, it appears that the effect of increase in conversion time can be only qualitatively explained. Quantitative predictions must await for good data on heat transfer coefficients at low *Gr* and *Re*.

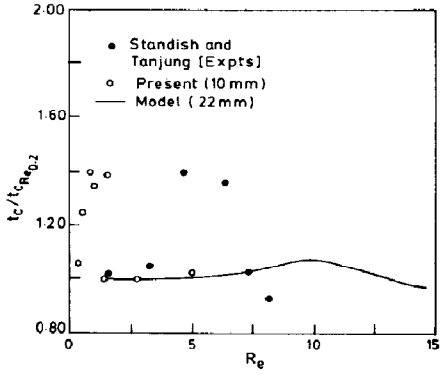

Fig. 8. The effect of Reynolds number on the conversion time for 10 mm char spheres (present) and 22 mm char spheres (Standish and Tanjung).

4. CONCLUSIONS

The present study has considered modelling the char conversion with CO_2 in spherical geometry as well as some critical experiments. The model based on conservation equations with detailed reaction–diffusion considerations have shown that it is possible to explain the conversion time vs diameter dependence, and conversion vs composition and, in part, temperature dependence. The kinetic limit for wood char appears to be around 100–250 μm, depending on the CO_2 content of the surrounding medium. The kinetic model used can be simplified by ignoring the reverse rate, but not any term in the denominator. Although the present work has concentrated on CO_2, the model is ready to be used to explain char conversion with mixtures involving O_2, CO_2 and N_2. Obtaining realistic predictions of dependence of flow effects must wait for the availability of good heat transfer data.

NOTATION

d_0	initial diameter, m
D	diffusion coefficient, m^2/s
$\tilde{D}$	effective diffusivity
E_s	superficial activation energy defined in eq. (16), kJ/mol
E	activation energy defined in eq. (1), kJ/mol
H_c	heat of combustion of carbon, kJ/kg
k	thermal conductivity, W/m^2 K
k_c	thermal conductivity of carbon (char), W/m^2 K
$\bar{k}$	thermal conductivity of porous char, W/m^2 K

k_1–k_4	reaction rate constants as in eq. (1)
Le	Lewis number ($= D\rho c_p/k$)
$\dot{m}$	mass flow rate of gas from solid, kg/s
M_i	molecular weight of the species, i, kg/kmol
Nu	Nusselt number
r	radial coordinate
r_p	pore radius in char, m
R	universal gas constant, J/kg mol K
$\dot{R}''$	radiation flux, W/m^2
S_g	surface area per unit volume of char, m^2/m^3
S_{g0}	surface area per unit volume of char at 0% conversion, m^2/m^3
t	time, s
T	temperature, K
Y_i	mass fraction of species i

Greek letters

ε	porosity
ρ	density of gas, kg/m^3
$\bar{\rho}$	density of porous char, kg/m^3
ρ_c	density of non-porous char, kg/m^3
$\dot{\omega}_c'''$	volumetric reaction rate of carbon, kg/m^3 s
$\dot{\omega}_c''$	reaction rate of carbon per unit area, kg/m^2 s

Subscripts

$i = 1, 2, 3$	species CO, CO_2 and N_2
s	surface
∞	free stream

REFERENCES

Anon, 1934, *Gas Engineers' Handbook*. McGraw-Hill, New York.

Blackwood, J. D. and Ingeme, A. J., 1960, The reaction of carbon with carbon dioxide at high pressure. *Aust. J. Chem.* **13**, 194–209.

Blackwood, J. D. and Mcgrory, F., 1958, The carbon–steam reaction at high pressure. *Aust. J. Chem.* **11**, 16–23.

DeGroot, W. F. and Shafizadeh, F., 1984, Kinetics of gasification of douglas fir and cottonwood chars by carbon dioxide. *Fuel* **63**, 210–216.

Dutta, S., Wen, C. Y. and Belt, R. J., 1977, Reactivity of coal and char. 1. In carbon dioxide atmosphere. *Ind. Engng Chem. Process Des. Dev.* **16**(1), 20–30.

Ergun, S., 1956, Kinetics of the reaction of carbon dioxide with carbon. *J. phys. Chem.* **60**, 480–485.

Gavalas, G. R., 1981, Analysis of char combustion including the effect of pore enlargement. *Combust. Sci. Technol.* **24**, 197–210.

Goldman, J., Xieu, D., Oko, A., Milne, R. and Essenhigh, R. H., 1984, A comparison of prediction and experiment in the gasification of anthracite in air and oxygen-enriched/steam mixtures, in *Proceedings of the 20th International Symposium on Combustion*, pp. 1365–1372. The Combustion Institute.

Groeneveld, M. J., 1980, The co-current moving bed gasifier. Ph.D. thesis, Twente University of Technology, The Netherlands.

Groeneveld, M. J. and van Swaaij, W. P. M., 1980, Gasification of char particles with CO_2 and H_2O. *Chem. Engng Sci.* **35**, 307–313.

Howard, J. B., 1967, Combustion of carbon with oxygen. Technical report, Massachusetts Institute of Technology.

Jaluria, Y., 1980, *Natural Convection Heat and Mass Transfer*. Pergamon, Oxford.

Jose, I., Amundson, N. R. and Park, S. K., 1990, Dynamics of a single particle during char gasification. *Chem. Engng Sci.* **45**, 387–401.

Kasaoka, S., Sakata, Y., Shimada, M. and Matsutomi, T., 1985, A new kinetic model for temperature programmed thermogravimetry and its applications to the gasification of coal chars with steam and carbon dioxide. *J. chem. Engng Japan* **18**(5), 426–432.

Mukunda, H. S., Paul, P. J., Srinivasa, U. and Rajan, N. K. S., 1984, Combustion of wooden spheres—experiments and model analysis, in *Proceedings of the 20th International Symposium on Combustion*, pp. 1619–1628, The Combustion Institute.

Mulhen, H. J., Heek, K. H. and Juntgen, H., 1985, Kinetic studies of steam gasification of char in the presence of H_2, CO_2 and CO. *Fuel* **64**, 944–949.

Reyes, S. and Jensen, K. F., 1986a, Percolation concepts in modelling of gas–solid reactions—I. Application to char gasification in kinetic regime. *Chem. Engng Sci.* **41**, 333–343.

Reyes, S. and Jensen, K. F., 1986b, Percolation concepts in modelling of gas–solid reactions—II. Application to char gasification in diffusion regime. *Chem. Engng Sci.* **41**, 345–354.

Satyanarayana, K. and Keairns, D. L., 1981, Study of kinetics of carbon gasification reactions. *Ind. Engng Chem. Fundam.* **20**, 6–13.

Simons, G. A., 1981, Comment on "analysis of char combustion including the effect of pore enlargement". *Combust. Sci. Technol.* **24**, 211–213.

Standish, N. and Tanjung, A. F. A., 1988, Gasification of single wood charcoal particles in CO_2. *Fuel* **67**, 666–672.

Sundaresan, S. and Amundson, N. R., 1979, Studies in char gasification—I. A lumped model. *Chem. Engng Sci.* **14**, 345–354.

Yuge, T., 1960, Experiments on heat transfer from spheres including combined natural and forced convection. *J. Heat Transfer Trans. ASME* **C82**, 214–220.